A global analysis searching for neutrinos associated with black hole merger gravitational wave events

Yu-Zi Yang[1], Jia-Jie Ling[1]⋆, Wei Wang[1] and Zhao-Kan Cheng[2]

[1] School of Physics, Sun Yat-sen University, Guangzhou 510275, China; *yangyz6@mail2.sysu.edu.cn,*
    lingjj5@mail.sysu.edu.cn, wangw223@mail.sysu.edu.cn
[2] School of Science, Harbin Institute of Technology, Harbin 150001, China; *14B911018@hit.edu.cn*

Abstract Several neutrino observatories have searched for coincident neutrino signals associated with gravitational waves induced by the merging of two black holes. No statistically significant neutrino signal in excess of the background level was observed. These experiments use different neutrino detection technologies and are sensitive to various neutrino types. A combined analysis was performed on the KamLAND, Super-Kamiokande and Borexino experimental data with a frequentist statistical approach to achieve a global picture of the associated neutrino fluence. Both monochromatic and Fermi-Dirac neutrino spectra were assumed in the calculation. The final results are consistent with null neutrino signals associated with the process of a binary black hole merger. The derived 90% confidence level upper limits on the fluence and luminosity of various neutrino types are presented for neutrino energy less than 110 MeV.

Key words: gravitational wave — black hole merger — neutrino fluence — global analysis

1 INTRODUCTION

After the detections of gravitational waves (GWs) released from black hole-black hole (BH-BH) mergers in 2015 by the Advanced Laser Interferometer Gravitational-wave Observatoy (LIGO) (LIGO Scientific Collaboration et al. 2015), many efforts have been made to search for coincident signals in astronomical observations. No significant counterpart was identified except for a coincident gamma-ray burst which was observed by the *Fermi Gamma-ray Space Telescope* (Connaughton et al. 2016) at ∼ 0.4 seconds after the GW150914 observation (Abbott et al. 2016b). In general, there is no theory of neutrino generation associated with BH-BH mergers. However, some physical phenomena, such as gravitational radiation, the synthesis of heavy elements and short gamma-ray bursts, are closely tied to the emission of neutrinos from BH accretion disk systems (Caballero et al. 2016). In the accretion disk system theory, neutrinos play a crucial role in setting the initial electron fraction of the outflow matter (Surman et al. 2008). Neutrino anni-

hilation can increase the prevalence of gamma-ray bursts (Popham et al. 1999). The appearance of a gamma-ray burst implies the accretion disk system theory may also work for BH-BH mergers. The search for GWs, gamma-ray bursts and neutrinos can open a new window for multi-messenger research into BH-BH mergers. This will lead to a more complete understanding of cosmic processes through a combination of information from different probes, and increase search sensitivity over any single detection method (Adrián-Martínez et al. 2016).

Two observed GW events in 2015 were both generated by the coalescence of binary BHs into a single BH. The first event, GW150914 (Abbott et al. 2016c), was observed on 2015 September 14. Two initial BHs with mass $36^{+5}_{-4}\,M_\odot$ and $29^{+4}_{-4}\,M_\odot$, at a luminosity distance of 410^{+160}_{-180} Mpc from the Earth, merged into a final BH with mass $62^{+4}_{-4}\,M_\odot$, radiating $3^{+0.5}_{-0.5}\,M_\odot$ away in the form of GWs. The second one, GW151226 (Abbott et al. 2016a), was observed on 2015 December 26. Masses of the two initial BHs were $14.2^{+8.3}_{-3.7}\,M_\odot$ and $7.5^{+2.3}_{-2.3}\,M_\odot$, and the mass of the final BH was $20.8^{+6.1}_{-1.7}\,M_\odot$. The source was located at a distance of 440^{+180}_{-190} Mpc from the Earth.

⋆ Corresponding author.

2 EXPERIMENTAL SEARCHES

Several neutrino observatories, including Super-Kamiokande (Super-K), KamLAND, Borexino, ANTARES, IceCube and Pierre Auger, have tried to search for neutrino signals associated with the two BH merger events. Since the neutrino generation mechanism from the merger of two BHs is still unclear, all of those experiments conservatively choose a ± 500 second coincidence time window centered around the GW observation time. More details about those experimental searches are introduced in the following paragraphs.

The KamLAND experiment (Gando et al. 2016) is located under 2700 meter water equivalent (m.w.e.) of vertical rock, below Mt. Ikenoyam in Gifu prefecture of Japan. The detector consists of a stainless-steel sphere and EVOH/nylon outer balloon. The outer balloon encloses a 1 kton liquid scintillator (LS). During GW150914, a mini-balloon was placed at the center of the detector to search for neutrinoless double beta decay. KamLAND focuses on the search for electron antineutrinos which are mainly detected through the inverse beta decay (IBD) reaction: $\bar{\nu}_e + p \rightarrow e^+ + n$. The coincidence of prompt (e^+ – ionization and annihilation) and delayed (n – capture on hydrogen) signals efficiently suppresses the backgrounds. The prompt signal has a strong bound with energy of $\overline{\nu}_e$, where $E_{\text{Prompt}} \approx E_\nu - 0.8\,\text{MeV}$. However, there are two major drawbacks. One is the loss of information about low energy $\bar{\nu}_e$ below the IBD interaction threshold, around 1.8 MeV. Another is the obscuration of information about the incoming neutrino's direction due to diffusion of the recoil neutrons. During the periods of GW150914 and GW151226, no neutrino candidates were detected by KamLAND.

Borexino (Agostini et al. 2017) is also an LS experiment located underground at 3400 m.w.e. in Gran Sasso National Laboratory, Italy. Besides the IBD detection channel, Borexino is also capable of detecting neutrinos via electron scattering (ES) thanks to its high purity scintillator with extremely low radioactive backgrounds. In comparison with the IBD method, ES does not have an energy threshold and is sensitive to all flavors of active neutrinos ($\overset{(-)}{\nu}_e$, $\overset{(-)}{\nu}_\mu$ and $\overset{(-)}{\nu}_\tau$). However, it is still challenging for an LS detector to determine the incoming neutrino direction by reconstructing the scattered electron with scintillator light. In the two GW periods, no neutrino signal was found in the IBD channel and one signal candidate was detected in the ES channel.

The Super-K experiment (Abe et al. 2016) has a large 50 kton water Cherenkov detector located at 2700 m.w.e.

underground in Kamioka, Japan. After a neutrino interacts inside of the detector, the Cherenkov ring pattern reconstruction can identify the final product of the charged particles, from which researchers at this facility can infer the neutrino's direction, flavor and energy. Neutrinos with energies from 3.5 MeV to 79.5 MeV are categorized as the "low energy data sample" which are typically solar neutrinos and supernova relic neutrinos. Data sets with energies above 100 MeV are typically used to study atmospheric neutrinos and search for proton decay. Because of its relatively "high energy" detection threshold, observable signals in the Super-K detector only originate from charged particles, which are positrons and electrons from IBD and ES interactions respectively. For that reason, Super-K is unable to separate these two kinds of interactions. Four neutrino candidates were observed by Super-K for GW150914 but no candidate was observed for GW151226.

Researchers working with the IceCube and ANTARES experiments (Adrián-Martínez et al. 2016) have also searched for coincident neutrino candidates in their recorded data. These projects are primarily sensitive to neutrinos with $\gg$ GeV energies. During the GW150914 and GW151226 periods, three neutrino candidates were found for each GW event, however these signals do not satisfy the spatial and temporal requirements.

3 GLOBAL ANALYSIS

As introduced above, with different detection technologies, different neutrino experiments are sensitive to different neutrino flavors and energy ranges. Performing a global analysis on those experimental data can produce a full picture of the BH merger coincident neutrino searches. Based on limited available information from publications, a global analysis was done with the "low energy" data samples from the Super-K, KamLAND and Borexino experiments, which are sensitive to neutrino energy less than 110 MeV.

Before performing a combined analysis, it is essential to understand each experiment's data and reproduce their results. Given the candidates with low reported statistical signal and background estimation, a maximum likelihood ratio method based on Poisson statistics is adopted to estimate the corresponding neutrino signal.

$$\chi^2(\mu) = 2\left[(\mu + n_{\text{bg}}) - n_{\text{obs}} + n_{\text{obs}} \cdot \ln \frac{n_{\text{obs}}}{\mu + n_{\text{bg}}}\right],$$
$$(1)$$

where μ is the number of expected neutrino signals from the BH-BH merger in the coincidence window, n_{bg} is

the estimated background and n_{obs} is the number of observed coincidence candidates.

Since all of those experiments did not observe any statistically significant neutrino signals, the estimated neutrino signals are consistent with zero. More importantly, as reported by those experiments, we also calculate N_{90}, which is the upper limit on the neutrino signal at the 90% confidence level (C.L.). Because of low event statistics, the traditional confidence interval setting method based on Wilks' theorem (Wilks 1938) is inaccurate. The Feldman-Cousins method (Feldman & Cousins 1998), based on a toy Monte Carlo simulation, is chosen to estimate the upper limit on the detected neutrino signal. Specifically, for each value of μ, 90% of the toy Monte Carlo events have smaller $\chi^2(\mu) - \chi^2(\mu_{\text{best}})$ values than $\Delta\chi^2_{90}(\mu)$, where μ_{best} is the best-fit value. The value of $\Delta\chi^2_{\text{data}}(\mu)$ was also calculated for each μ using the actual number of observed candidates in the experimental data. N_{90} equals the maximal values of μ when $\Delta\chi^2_{\text{data}}(\mu) \leq \Delta\chi^2_{90}(\mu)$.

As shown in Table 1, our reproduced neutrino signal upper limits are consistent with the reported experimental results.

The upper limit on the signal N_{90} can be converted into the upper limit on neutrino fluence, F_{UL}, which is the neutrino flux at the Earth. The calculation formula is given by

$$F_{\text{UL}} = \frac{N_{90}}{N_T \int \phi(E_\nu)\sigma(E_\nu)\epsilon(E_\nu)dE_\nu} , \quad (2)$$

where N_T stands for the total number of target nuclei, which are protons that participate in IBD interactions and electrons in ES. $\phi(E_\nu)$ is the normalized neutrino energy spectrum, $\epsilon(E_\nu)$ is the total detection efficiency, including the time window selection efficiency, detection efficiency, etc. $\sigma(E_\nu)$ is the neutrino interaction cross section. The IBD cross section is taken from Strumia & Vissani (2003); while the ES differential cross section is shown in Equation (3) (Giunti & Chung 2007).

$$\frac{d\sigma(E_\nu, T_e)}{dT_e} = \frac{2G_F^2 m_e^2}{\pi}$$
$$\times \left[g_1^2 + g_2^2 \left(1 - \frac{T_e}{E_\nu}\right)^2 - g_1 g_2 \frac{m_e T_e}{E_\nu^2} \right], \quad (3)$$

where G_F is the Fermi constant, m_e is the electron mass and T_e is the kinetic energy of the recoil electron. E_ν stands for neutrino energy. g_1, g_2 are the coupling constants: $g_1^{(\nu_e)} = g_2^{(\bar{\nu}_e)} = \frac{1}{2} + \sin^2\theta_W$ and $g_2^{(\nu_e)} = g_1^{(\bar{\nu}_e)} = \sin^2\theta_W$ for electron type neutrinos (anti-neutrinos), where θ_W is the Weinberg angle;

$g_1^{(\nu_{\mu,\tau})} = g_2^{(\bar{\nu}_{\mu,\tau})} = -\frac{1}{2} + \sin^2\theta_W$ and $g_2^{(\nu_{\mu,\tau})} = g_1^{(\bar{\nu}_{\mu,\tau})} = \sin^2\theta_W$ for muon or tau type neutrinos (antineutrinos).

For a global analysis, the expected number of neutrino signals at various experiments are different due to differing target mass, interaction cross section and detection efficiencies. Instead, we can directly introduce neutrino fluence, F, in the total $\chi^2(F)$ as shown in Equation (4)

$$\chi^2(F) = \sum_i^{\text{exps}} \chi_i^2(F)$$
$$= 2 \sum_i^{\text{exps}} \left[(F \cdot N_T \cdot \sigma_{\text{eff},i} + n_{\text{bg},i}) - n_{\text{obs},i} \right. \quad (4)$$
$$\left. + n_{\text{obs},i} \cdot \ln \frac{n_{\text{obs},i}}{F \cdot N_T \cdot \sigma_{\text{eff},i} + n_{\text{bg},i}} \right],$$

where $\sigma_{\text{eff},i}$ is the effective cross section embedded in the detector efficiency of the i-th experiment, which is defined as

$$\sigma_{\text{eff},i} = \int \phi(E_\nu)\sigma(E_\nu)\epsilon(E_\nu)dE_\nu . \quad (5)$$

Hence the upper limits for neutrino fluence F_{UL} can also be computed using the Feldman-Cousins method, similar to calculation of the upper limit for the neutrino signal N_{90}, as described previously. The systematic correlations among those measurements are negligible except for the theoretical model of neutrino production from BH-BH mergers, which are independent of experimental measurement.

Since the neutrino energy spectrum $\phi(E_\nu)$ is unclear, the upper limits for neutrino fluence were calculated using two hypotheses: monochromatic and Fermi-Dirac distributions.

3.1 Monochromatic Energy Spectrum

The simplest hypothesis for the neutrino energy spectrum assumes all neutrinos have the same energy and follow a $\delta(E_\nu)$ distribution. This assumption provides the most conservative (or the largest) upper limits on neutrino fluence at a given neutrino energy E_ν.

Two global analyses were done. One only included the two largest LS experiments (KamLAND and Borexino), because LS detectors have high sensitivities to low energy $\bar{\nu}_e$ detection. The other included all three experiments. The 90% C.L. upper limits on $\bar{\nu}_e$ neutrino fluence with respect to neutrino energy for GW150914 and GW151226 BH-BH mergers are shown in Figure 1. The combined upper limits on $\bar{\nu}_e$ fluence are from $1.0 \times$

Table 1 Experimental results from KamLAND, Borexino and Super-K neutrino observatories on GW150914 (GW151226), including the detection method, neutrino energy ranges, signal candidates, background estimations, and both the published and reproduced 90% C.L. upper limits on signal N_{90}.

Experiment	Channel	Energy (MeV)	ν Candidates	Backgrounds	N_{90} (Published)	N_{90} (Reproduced)
KamLAND	IBD	1.8–110	0 (0)	0.18 (0.02)	2.26 (2.41)	2.25 (2.41)
Borexino	IBD	1.8–75	0 (0)	$\sim$0 ($\sim$0)	2.44 (2.44)	2.43 (2.43)
	ES	0.4–15	0 (1)	1.68 (1.72)	N/A	1.3 (2.8)
Super-K	IBD/ES	3.5–79.5	4 (0)	2.90 (2.90)	5.41 (2.30)	5.92 (1.0)

Notes: Super-K used Bayesian statistical methods to calculate the upper limits on neutrino signals (Abe et al. 2016). We recalculate their results with the frequentist Feldmen-Cousins approach. Borexino does not report the N_{90} result on the EC channel.

$10^{12}\,\mathrm{cm}^{-2}$ to $1.6 \times 10^{7}\,\mathrm{cm}^{-2}$ (from $1.0 \times 10^{12}\,\mathrm{cm}^{-2}$ to $2.9 \times 10^{6}\,\mathrm{cm}^{-2}$) for GW150914 (GW151226) at the energy range ($1.8\,\mathrm{MeV} < E_\nu < 79.5\,\mathrm{MeV}$). Since the IBD cross section is proportional to E_ν^2, the corresponding neutrino fluence is inversely proportional to E_ν^2 according to Equation (2). For extremely low energy neutrinos ($E_\nu < 1.8\,\mathrm{MeV}$), the resulting sensitivity only comes from the Borexino experiment through the ES interaction channel; for low energy neutrinos ($1.8\,\mathrm{MeV} < E_\nu < 5\,\mathrm{MeV}$), LS experiments, especially KamLAND, contribute mainly to the sensitivity due to a larger IBD cross section; while for neutrino energy ($5.0\,\mathrm{MeV} < E_\nu < 79.5\,\mathrm{MeV}$), Super-K dominates the sensitivity due to its huge target mass.

The fluence of other types of neutrinos, ν_e and ν_x (ν_μ and ν_τ), can only be deduced from the ES channel. As shown in Figure 2, the combined 90% C.L. upper limits for ν_e, ν_x fluence are from $1.7 \times 10^{13}\,\mathrm{cm}^{-2}$ to $1.6 \times 10^{9}\,\mathrm{cm}^{-2}$ and from 7.7×10^{13} to $1.0 \times 10^{10}\,\mathrm{cm}^{-2}$ respectively for GW150914 at the energy range of $1.0\,\mathrm{MeV} < E_\nu < 79.5\,\mathrm{MeV}$. For GW151226, the obtained upper limits are from $3.6 \times 10^{13}\,\mathrm{cm}^{-2}$ to $2.8 \times 10^{8}\,\mathrm{cm}^{-2}$ and from $1.6 \times 10^{14}\,\mathrm{cm}^{-2}$ to $1.7 \times 10^{9}\,\mathrm{cm}^{-2}$ for ν_e and ν_x respectively. According to Equation (3), the ratio of $\sigma_{\nu_e}/\sigma_{\bar{\nu}_e} \simeq 2.5$, so the upper limits on ν_e and $\bar{\nu}_e$ fluence from Borexino are similar. However, $\sigma_{\nu_e,\mathrm{ES}}$ is about two orders of magnitude lower than $\sigma_{\bar{\nu}_e,\mathrm{IBD}}$, therefore the resulting upper limit on ν_e would be two orders of magnitude higher than $\bar{\nu}_e$'s in the Super-K experiment.

3.2 Fermi-Dirac Energy Spectrum

During a binary BH merging process, the neutrino released may obey the Fermi-Dirac energy distribution with zero chemical potential $\eta = 0$

$$\phi_{\mathrm{Fermi-Dirac}}(E_\nu) = \mathrm{Norm} \cdot \frac{E_\nu^2}{1 + e^{E_\nu/T - \eta}}, \quad (6)$$

where 'Norm' stands for a normalization factor and T is the effective neutrino temperature, which is set to be 5 MeV as the nominal value.

The 90% C.L. upper limits on integrated ν_e, $\bar{\nu}_e$ and ν_x fluence and luminosity obtained from KamLAND, Borexino and Super-K experiments, and their combined results, are shown in Tables 2 and 3, where the luminosity L is the total released energy taken by neutrinos during a BH-BH merging process. It can be calculated using the $L = F \cdot 4 \cdot \pi \cdot D_{\mathrm{gw}}^2 \cdot \langle \bar{E} \rangle$ equation, where D_{gw} is the distance from the GW source to the Earth and $\langle \bar{E} \rangle$ is the average neutrino energy which equals $3.15 \cdot T$. Since the uncertainties of the measured distances for those GW events are quite large, luminosity is written as a function of the true distance to the source

$$L_{\mathrm{GW150914}} = L_0 \left(\frac{D_{\mathrm{gw}}}{410\mathrm{Mpc}} \right)^2 \mathrm{erg} \quad (7)$$

and

$$L_{\mathrm{GW151226}} = L_0 \left(\frac{D_{\mathrm{gw}}}{440\mathrm{Mpc}} \right)^2 \mathrm{erg} . \quad (8)$$

As shown in Figure 3, 90% C.L. upper limits on the combined ν_e, $\bar{\nu}_e$ and ν_x neutrino fluence obtained from the Fermi-Dirac energy distribution are shown with respect to the effective neutrino temperature T. As T increases, the averaged neutrino energy will also increase, which results in a larger neutrino interaction cross section. As a result, the derived neutrino fluence will decrease with respect to T as shown in Equation (2).

4 DISCUSSION

In this analysis, each GW event is calculated separately. If the mechanism of neutrino generation from a BH-BH merger process is the same, these GW events can be analyzed together with some assumptions on their origin. The neutrino fluence may be proportional to the mass of two merger BHs or the mass of a remnant relic, and its velocity of rotation. It is not clear whether the release of neutrinos occurs at the merger phase or cooling phase.
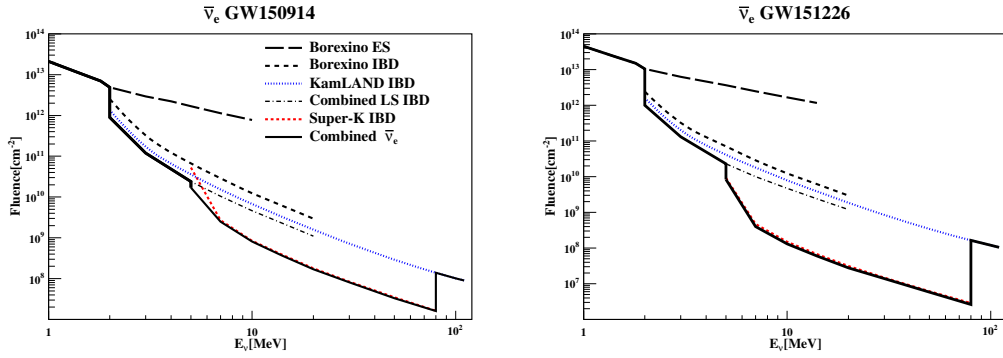
Fig. 1 The 90% C.L. upper limits on $\bar{\nu}_e$ fluence from GW150914 and GW151226 BH-BH mergers with respect to the monochromatic neutrino energy E_ν. The *dot-dashed line* represents the combined analysis result for KamLAND and Borexino while the *solid line* represents the global analysis result based on all three experiments.
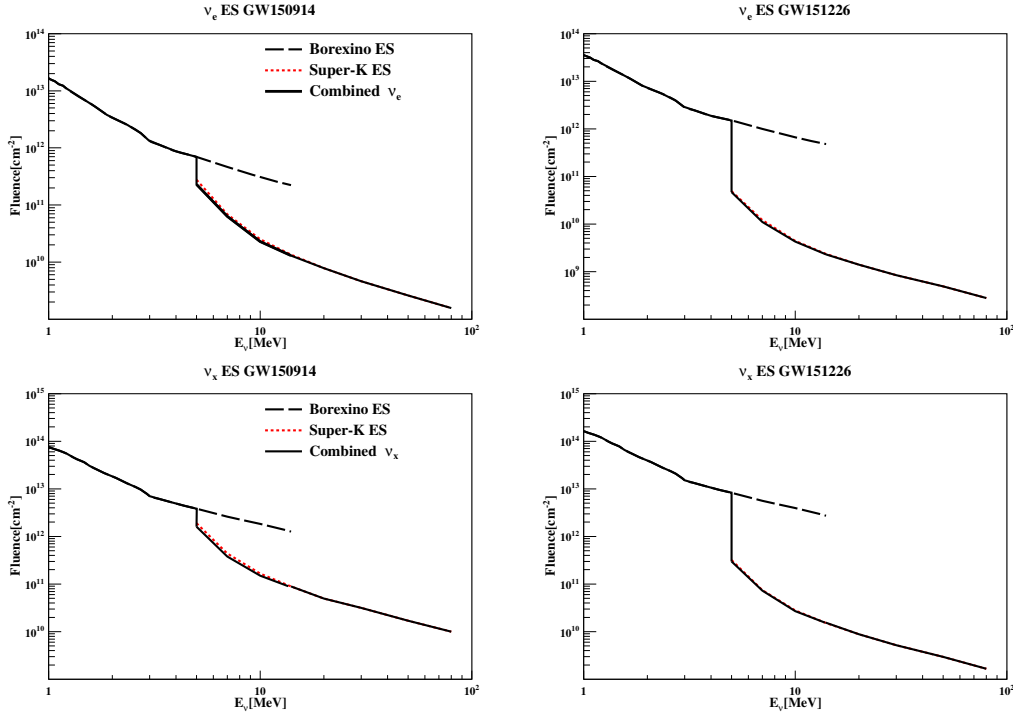

Fig. 2 The 90% C.L. upper limits on ν_e and ν_x fluence from GW150914 and GW151226 BH-BH mergers as a function of the monochromatic neutrino energy E_ν.
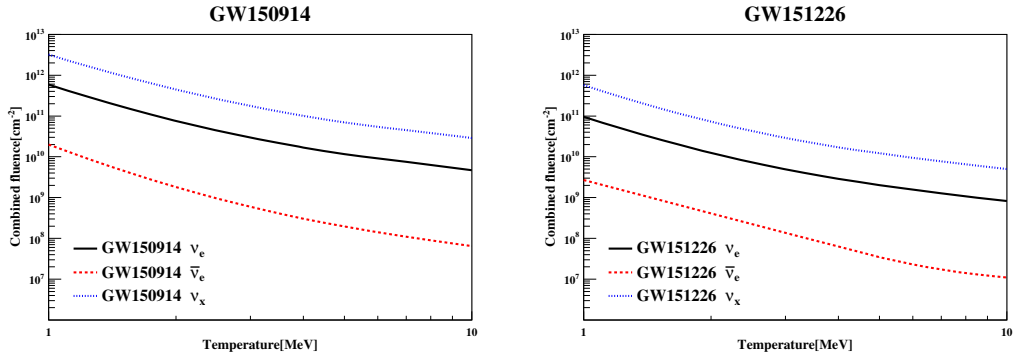

Fig. 3 The 90% C.L. upper limits on neutrino fluence for GW150914 and GW151226 for various types based on the Fermi-Dirac energy spectrum with respect to effective neutrino temperature T.

Table 2 The 90% C.L. upper limits on ν_e, $\bar{\nu}_e$ and ν_x fluence from Borexino, KamLAND and Super-K experiments, and the combined results for GW150914 (GW151226).

Experiment	90% C.L. F_{UL} (cm^{-2})		
	ν_e	$\bar{\nu}_e$	ν_x
KamLAND	-	2.0×10^9 (2.4×10^9)	-
Borexino	3.4×10^{11} (7.4×10^{11})	2.7×10^9 (2.7×10^9)	1.9×10^{12} (4.1×10^{12})
Super-K	1.2×10^{10} (2.0×10^9)	2.6×10^8 (4.0×10^7)	7.2×10^{10} (1.2×10^{10})
Combined	1.2×10^{10} (2.0×10^9)	2.2×10^8 (3.7×10^7)	7.1×10^{10} (1.2×10^{10})

Table 3 The 90% C.L. upper limits on ν_e, $\bar{\nu}_e$ and ν_x neutrino luminosity from Borexino, KamLAND and Super-K experiments, and the combined results for GW150914 (GW151226) without oscillation.

Experiment	90% C.L. L_{0UL} (erg)		
	ν_e	$\bar{\nu}_e$	ν_x
KamLAND	-	1.0×10^{60} (1.4×10^{60})	-
Borexino	1.7×10^{62} (4.3×10^{62})	1.4×10^{60} (1.6×10^{60})	9.6×10^{62} (2.4×10^{63})
Super-K	6.1×10^{60} (1.2×10^{60})	1.3×10^{59} (2.4×10^{58})	3.6×10^{61} (6.9×10^{60})
Combined	6.1×10^{60} (1.2×10^{60})	1.2×10^{59} (2.2×10^{58})	3.6×10^{61} (6.9×10^{60})

That will also affect the arrival time of the neutrino signals relative to the corresponding GW signal. In addition, at this stage the uncertainties associated with the BH masses and distances from the Earth are quite large. More precise measurements with more statistical analysis in the future will be very helpful for further study on this topic. It will help us to understand the physics behind BH-BH mergers, as well as the underlying neutrino physics.

5 CONCLUSIONS

A global analysis was performed on experimental data from the KamLAND, Super-K and Borexino experiments to search for neutrinos associated with GW150914 and GW151226 events with a frequentist statistical approach. The final results are consistent with null neutrino signals associated with the process of a binary BH mergers. For GW150914, the obtained 90% C.L. upper limits on $\bar{\nu}_e$, ν_e and ν_x fluence are from 2.1×10^{13} cm^{-2} to 1.6×10^7 cm^{-2}, from 1.7×10^{13} cm^{-2} to 1.6×10^9 cm^{-2} and from 7.7×10^{13} cm^{-2} to 1.0×10^{10} cm^{-2} in the energy range of 1.0 MeV $< E_\nu < 79.5$ MeV, assuming a monochromatic energy spectrum; while assuming a Fermi-Dirac energy spectrum with an effective temperature of 5 MeV, the combined 90% C.L. upper limits on ν_e, $\bar{\nu}_e$ and ν_x fluence are 1.2×10^{10} cm^{-2}, 2.2×10^8 cm^{-2} and 7.1×10^{10} cm^{-2} respectively. Similar results are also obtained for GW151226 with slightly better upper limits.

References

Abbott, B. P., Abbott, R., Abbott, T. D., et al. 2016a, Physical Review Letters, 116, 241103

Abbott, B. P., Abbott, R., Abbott, T. D., et al. 2016b, ApJ, 826, L13

Abbott, B. P., Abbott, R., Abbott, T. D., et al. 2016c, Physical Review Letters, 116, 061102

Abe, K., Haga, K., Hayato, Y., et al. 2016, ApJ, 830, L11

Adrián-Martínez, S., Albert, A., André, M., et al. 2016, Phys. Rev. D, 93, 122010

Agostini, M., Altenmüller, K., Appel, S., et al. 2017, ApJ, 850, 21

Caballero, O. L., Zielinski, T., McLaughlin, G. C., & Surman, R. 2016, Phys. Rev. D, 93, 123015

Connaughton, V., Burns, E., Goldstein, A., et al. 2016, ApJ, 826, L6

Feldman, G. J., & Cousins, R. D. 1998, Phys. Rev. D, 57, 3873

Gando, A., Gando, Y., Hachiya, T., et al. 2016, ApJ, 829, L34 [Erratum: Astrophys. J. 2017, 851, L22]

Giunti, C., & Chung, W. K. 2007, Fundamentals of Neutrino Physics and Astrophysics (Oxford University Press)

LIGO Scientific Collaboration, Aasi, J., Abbott, B. P., et al. 2015, Classical and Quantum Gravity, 32, 074001

Popham, R., Woosley, S. E., & Fryer, C. 1999, ApJ, 518, 356

Strumia, A., & Vissani, F. 2003, Physics Letters B, 564, 42

Surman, R., McLaughlin, G. C., Ruffert, M., Janka, H.-T., & Hix, W. R. 2008, ApJ, 679, L117

Wilks, S. S. 1938, Annals Math. Statist., 9, 60